Viscous Inertial Shear-Transition-Adaptive (VISTA) Porous Media Head-Loss Formulation

Bruce Letellier[1], Mark Macali[1] and Ernie Kee[2]
[1]Alion Science and Technology, 6200 Uptown Blvd, NE, Albuquerque, NM, USA
[2]Texas A&M University, College Station, TX, USA
bletellier@alionscience.com

Classic head-loss formulas for pressure drop in porous media often have two terms that are linearly and quadratically proportional to velocity; $dP = a\mu v + b\rho v^2$. The first term represents Stokes' limit for viscous shear, and the second term represents Newton's limit for inertial drag. The practice of linearizing complex phenomena arising from molecular kinetics leads to simple addition of the two terms, which individually dominate widely separated flow regimes; but for application to porous media flow through debris beds that accumulate on emergency core cooling systems, the two-term approximation is not robust in the transition region. A new correlation method, Viscous Inertial Shear-Transition-Adaptive (VISTA) head loss is proposed that preserves both physical limits while adapting to the flow transition needed to best describe pressure drop through tested porous media. Most debris beds that accumulate on emergency recirculation strainers experience low-velocity flow transitions where neither of the traditional terms predicts head loss adequately, leading to complicated coefficients. Correlation of pressure loss data in terms of Reynolds number permits VISTA to compare, on an equal basis, seemingly disparate internal flow regimes using a compact formulation.

Theory is presented and the VISTA model is calibrated to head loss observed in compressible, fibrous, particulate-loaded media prototypical of composite debris beds found in nuclear safety applications. Strong correlation demonstrates potential benefit of the VISTA formulation. Although a familiar parameterization of internal drag area (surface-to-volume ratio) is employed, laboratory measurements for fiberglass and representative particulate are applied rather than traditional geometric approximations based on shape and size. The VISTA head-loss formula is coupled with a simple model for uniform bed compression that requires iterative solution between maximum and minimum compression limits. Under the assumption of uniform compression, factorized formulas isolate the effect of spatial variations in debris properties for convenient examination. In common with most classic head-loss treatments, the VISTA head-loss correlation does not address filtration and migration processes, so presumed or measured debris configurations must be available to calibrate free parameters.

I. VISTA HEAD-LOSS FORMULATION

Two fundamental elements of head-loss prediction in compressible porous media are developed in the following subsections. Section I.A reviews the physical processes of viscous shear and inertial drag that cause pressure drop in fluid flow through a porous debris bed and develops the basic differential equation that preserves limiting behavior while adapting to the Reynolds flow regime of interest. Section I.B incorporates a uniform compression model with new constraints on maximum compression and presents an iteration scheme for efficient solution of bed thickness and its corresponding pressure drop. Section II to follow discusses constitutive formulas needed to describe composite debris properties.

I.A. Differential Pressure Equation

The following derivation offers a mechanism for combining the effects of viscous shear and inertial drag in proper proportion supported by data. A familiar formula for inertial drag is derived first, followed by substitution of a generalized drag coefficient that is also capable of preserving the viscous limit. Additional details and discussion are provided in Ref. 1.

The initial point of view for deriving inertial drag (Newton limit) is one of external flow around a moving sphere where the rate of mass displacement equals the cross sectional area of the body times the velocity times the fluid density within the displaced volume, i.e., $\dot{m} = \rho \frac{\pi}{4} d^2 \bar{w}$. The acceleration of the displaced fluid is proportional to the relative velocity between the body and the fluid, so when the bulk fluid is at rest, $F_D = \frac{\text{change of momentum}}{\text{unit of time}} \propto \dot{m}\bar{w} = \rho \frac{\pi}{4} d^2 \bar{w}^2$. Thus, the force required to move the body through the medium, or equivalently, the drag exerted on the body as the fluid passes around it, is given by $F_D = K\rho \frac{\pi}{4} d^2 \bar{w}^2$ where K is a constant of proportionality.

Classic experiments show that the proportionality between drag force and momentum change is only approximately constant for spherical-particle Reynolds

numbers $Re > 1000$, so a more general convention is adopted by introducing a drag coefficient that can be correlated as a function of Re. The standard formula is

$$F_D = \frac{1}{2} C_D(Re) \frac{\pi}{4} \rho d^2 \bar{w}^2. \quad (1)$$

Figure 1 illustrates empirical behavior of the drag coefficient C_D that is typical for several standard debris-element geometries (spheres, disks, cylinders) over a wide range of Reynolds number.

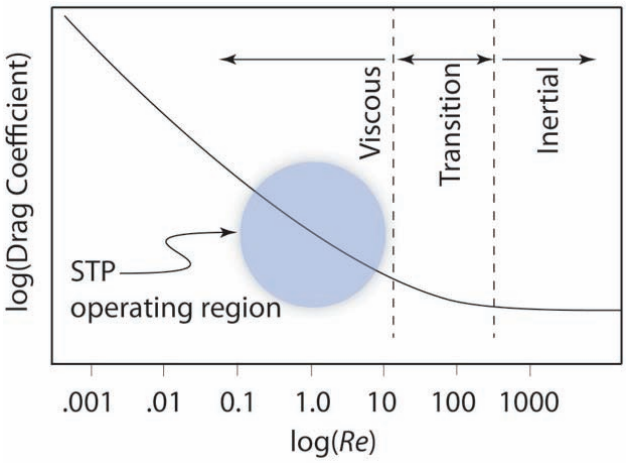

Fig. 1. Trend of measured drag coefficients typical for spheres, disks, and cylinders (stylized after Lapple[2]).

Eq. 1.0 describes the inertial drag force acting on individual debris elements by fluid moving through the bed. It is intuitively obvious that drag must be exerted along the surface of all debris that is in contact with moving fluid, so many similarities arise with the treatment of viscous shear coupled to the walls of a capillary flow channel. In fact, the standard treatment is to define an inertia-induced drag stress analogous to viscous stress such that

$$\tau_{Drag} = \frac{F_D}{A_{particle}} = \frac{R}{2}\left(\frac{dP}{dz}\right)_{Drag}, \quad (2)$$

where R is the effective radius of a typical flow path that will be related to a characteristic dimension called the hydraulic radius. One important question that arises immediately is, what area $A_{particle}$ should be used to distribute the drag force? Viscous shear, which should dominate flow regimes of interest for most emergency strainers, is generally assumed to affect the entire surface of the debris; so for now, it is reasonable to assume that inertial drag can also be distributed across the entire debris surface. However, it should be noted that conventional definitions of the drag coefficient like Eq. 1 have sometimes been scaled by the cross sectional area of obstacles presented to the flow. Distribution of drag force over the entire interior surface area of a porous bed will introduce different empirical factors that should be determined by fits to data.

Reversing the sign of Eq. 2 to account for inertial drag acting on a fluid element, substitution into Eq. 1, and solving for the pressure gradient leads to the relation

$$-\left(\frac{dP}{dz}\right)_{Drag} = \frac{2}{A_{particle} R}\left[\frac{1}{2} C_D(Re) \frac{\pi}{4} \rho d^2 \bar{w}^2\right]. \quad (3)$$

The area of the spherical particle used as an illustration for drag force is $A_{particle} = \pi d^2$, which eliminates the same product from the square brackets. Assuming that the total volumetric flow rate is constant throughout the bed (mass conservation) allows factoring the local average velocity in terms of the strainer face approach velocity, $\bar{w}^2 = w_A^2/\varepsilon^2$, where ε is the local porosity. Finally, the characteristic length for internal flow (called the hydraulic radius) is defined as

$$R_H = \frac{\text{fluid volume}}{\text{debris area}} = \frac{\varepsilon \forall}{(1-\varepsilon)\forall S_V} = \frac{\varepsilon}{(1-\varepsilon) S_V}, \quad (4)$$

where $\forall$ is an arbitrary debris volume, ε is the local porosity, $(1-\varepsilon)$ is the local solidity, and S_V is the ratio of debris surface area to debris solid volume. For a cylindrical capillary, the effective radius $R = 2R_H$. Substituting these relationships in Eq. 3 gives

$$-\left(\frac{dP}{dz}\right)_{Drag} = \frac{1}{8} C_D(Re)\left(\frac{1-\varepsilon}{\varepsilon^3}\right) S_V \rho w_A^2. \quad (5)$$

The discussion of composite debris properties in Section II proposes a further substitution for the surface-to-volume ratio $S_V = \rho^{mat} S_A$ where ρ^{mat} is the material density of a debris constituent and S_A is the specific surface area $\{area/mass\}$ of the constituent obtained by direct laboratory measurement. Note that in its most basic form, the hydraulic scaling stated by Eq. 5 assumes that the entire surface area of the debris participates in the flow, not just the surface area that is aligned perpendicular to the flow. Other scaling arguments have been proposed that introduce shape factors for high-porosity filter media[3], but the present approximation is sufficient to demonstrate the VISTA methodology.

Only the form of the drag coefficient remains to be rationalized, and the empirical trend presented in Figure 1 suggests a deceptively simple opportunity for joint treatment of viscous shear and inertial drag. Note that the plots depict a smoothly behaved function of Reynolds number that can span up to 10 decades of magnitude. Reynolds number for internal flow relevant to debris beds varies between 0.1 and 10 where the dependence on Re is almost linear on the log-log scale. For this application, Reynolds number is defined as

$$Re = \frac{\rho \bar{w} R_H}{\mu} = \frac{\rho w_A}{\mu(1-\varepsilon) S_V} \frac{\varepsilon}{\varepsilon}. \quad (6)$$

The narrow range of Reynold's number internal to debris beds and regular variation of the drag coefficient with Reynold's number shown in Fig. 1 suggest that a floating power-law fit of the drag coefficient vs. Reynold's number (linear plot in log-log space) might have sufficient flexibility to match the physical limits posed by both viscosity (low Reynolds) and inertia (high Reynolds). Thus, the drag coefficient is assumed to be a generalized power law such that

$$C_D\left(Re\right)=\tilde{b}\left(Re\right)Re^{m(Re)}=\tilde{b}\left(Re\right)\left(\frac{\rho w_A}{\mu\left(1-\varepsilon\right)S_V}\right)^{m(Re)}, \quad (7)$$

so that Eq. 5 becomes

$$-\left(\frac{dP}{dz}\right)=b\left(\frac{\rho w_A}{\mu\left(1-\varepsilon\right)S_V}\right)^{m}\left(\frac{1-\varepsilon}{\varepsilon^3}\right)S_V\rho w_A^2, \quad (8)$$

where the integer constant has been subsumed in the empirical parameter and the differential pressure is now understood to represent the total change caused by all phenomena. This form permits the slope of the log-log approximation to "float" along the composite drag coefficient by fitting local values of $b\left(Re\right)$ and $m\left(Re\right)$. A fully calibrated correlation would define for a complex debris bed the tangent of an underlying drag coefficient that would look very much like Figure 1 over a limited range of Re.

Approximation of the drag coefficient using a power law defined in Re was first suggested by Reynolds in 1883, and Rott (18) recounts early use of power-law formulas for hydraulic studies in engineering and physics. In some sense, VISTA represents a return to the empirical roots of hydraulic pressure loss to describe the challenging transition zone where modern sump strainers with debris beds appear to operate. The convenience of modern data analysis permits the exponential value and leading coefficient to "adapt" to the local conditions by themselves being functions of the Reynolds number. This feature is the unique attribute that provides enough flexibility to span the viscous/inertial transition zone without sacrificing accuracy; whereas, the quadratic form can only trust eventual algebraic dominance between the two terms across the same range of conditions.

One essential benefit of parameterizing drag as a power law in Reynolds number is that limiting formulas for viscous and inertial drag can be recovered separately when Eq. 8 is evaluated with appropriate exponents. When $m=-1$, Eq. 8 reduces to the Kozeny-Carman viscous limit[4]

$$-\left(\frac{dP}{dz}\right)=b_{visc}\frac{\left(1-\varepsilon\right)^2}{\varepsilon^3}S_V^2\mu w_A. \quad (9)$$

When $m=0$, Eq. 8 reduces to the inertial limit[5]

$$-\left(\frac{dP}{dz}\right)=b_{drag}\left(\frac{1-\varepsilon}{\varepsilon^3}\right)S_V\rho w_A^2. \quad (10)$$

Any correlation of a debris bed with $-1<m<0$ will include an appropriate mixture of both viscous and inertial effects. One major advantage of the composite correlation is that the fitting parameters b and m are themselves functions of the Reynolds number that includes factors of both porosity and surface-to-volume ratio. Dependence of the parameters on bed properties should permit additional collapse of the geometry dependence exhibited in Fig. 1. In this sense, the correlation can "adapt" to the local flow conditions presented by prototypical debris beds. By comparison, the parameters of most head loss correlations are fixed numeric values. Test programs can easily span the desired range of Reynolds number by using any combinations of bed geometry, fluid velocity and fluid temperature. Confirmatory tests can then be conducted over the same span of Reynolds number using alternate factors that achieve the same hydraulic scaling to demonstrate that the VISTA head-loss correlation is robust over debris compositions and flow conditions relevant to ECCS strainer performance. Residual variation present in the parameters b and m, which will be manifest as a variation in tangent lines, can then be propagated using uncertainty distributions for risk-informed applications.

It is important to understand that all elements of Eq. 8 related to bed properties (namely ε, S_V, b, m) are spatially dependent and can vary with position within the debris. Fluid properties defined by μ, ρ, w_A are constant throughout the bed. Because Reynolds number depends on both fluid properties and local flow geometry, Re is also a function of bed location. Spatial properties are important for addressing questions regarding time-ordered bed stratification, and for examining local flow restrictions such as debris impaction inside of perforated plate orifices.

A particularly useful form of Eq. 8 is

$$-\left(\frac{dP}{dz}\right)=\frac{\rho^2 w_A^3}{\mu}\frac{b\left(z\right)}{\varepsilon\left(z\right)^3}Re\left(z\right)^{m(z)-1}, \quad (11)$$

where all fluid properties are collected as a leading coefficient that can be assumed constant throughout a debris bed and spatial dependencies are explicitly noted. Given spatial profiles for porosity and surface-to-volume ratio that are either assumed, measured or predicted by other models, Re is obtained from Eq. 6 and the drag coefficient parameters can be read from a calibration curve that is appropriate for the prototypical debris composition being studied.

If bed properties are uniform with little to no evidence of compression, then the direct integral of Eq. 11 gives the total pressure drop across a bed of thickness ΔL,

$$\Delta P=\frac{\rho^2 w_A^3}{\mu}\frac{b}{\varepsilon^3}\Delta L Re^{m-1}. \quad (12)$$

This result can be applied across any portion of a bed for which the stated assumptions are reasonable.

I.A. Bed Compression

Under hydraulic loads induced from moving fluid, thickness reduction observed in fibrous debris beds arises from two mechanisms: (1) compression, defined as fully recoverable tensile loading of the mechanical linkage between fibers; and (2) compaction, defined as irreversible relative motion of debris elements caused by local force imbalance that relieves tensile stress and results in internal reconfiguration. Both mechanisms reduce porosity. Under prolonged fluid flow, fibrous debris beds can settle via compaction mechanisms that prevent compressive recovery.

Internal hydraulic loads on the debris caused by viscous shear and inertial drag are transferred through physical contact between debris elements in a cumulative fashion very analogous to static hydrodynamic loads. Thus, debris elements near the bottom of the bed next to the strainer plate experience higher compressive loads than debris elements near the top of the bed. In the theoretical limit of a perfect linear spring, the nonuniform spatial distribution of porosity can be calculated analytically knowing only the spring constant and the local drag force as a function of position, which in turn depends on local compression in a positive feedback loop that iterates to an equilibrium configuration. With high particulate loads, it is doubtful that nonuniform fiber compression competes with particulate migration (compaction) as a dominant means of porosity reduction, so it is more common to apply uniform compression models that match total observed thickness reduction. Uniform compression is analogous to a spring loaded only from the top so that porosity reduction is constant throughout the bed.

Reference 6 recommends a uniform compression model that describes the ratio between mixed bed thickness ΔL_m and the theoretical reference thickness ΔL_0 in terms of the ratio between the manufactured packing density c_0 and the actual bed packing density c; $\Delta L_m / \Delta L_0 = c_0 / c$, where the manufactured density is approximately 2.4 $\text{lb}_\text{m}/\text{ft}^3$ and the maximum recommended particulate-loaded packing density is approximately $c_{max} = 65$ $\text{lb}_\text{m}/\text{ft}^3$. Although finely divided fiber beds are sometimes observed to have an effective thickness greater than the equivalent amount of manufactured insulation, it is reasonable to enforce the limits

$$1 \le \frac{\Delta L_0}{\Delta L_m} = \frac{c}{c_0} \le \frac{65}{2.4} = 27. \tag{13}$$

Based on work of Ingmanson[3], Reference 6 recommends a correlation for uniform bed compression of the form

$$\frac{\Delta L_m}{\Delta L_0} = \frac{c_0}{c} = \frac{1}{\tilde{a}}\left(\Lambda \frac{\Delta P}{\Delta L_0}\right)^{-\gamma}, \tag{14}$$

where $\tilde{a} \approx 1.3$ and $\gamma \approx 0.38$ are empirical constants, ΔP is the positive pressure *drop*, and $\Lambda = 8.5 \times 10^{-6}$ is the factor needed to convert from SI units of Pa/m to the correlation units of ft-h_2o/inch. Following formulas will factor the units conversion and substitute $a = \tilde{a}/\Lambda^{-\gamma}$ to simplify the notation.

Note that the ratio $\Delta P / \Delta L_0$ appearing in Eq. 14 represents the average pressure gradient that would be present if the same pressure drop were experienced across a bed with corresponding theoretical thickness. For the purpose of investigating non-uniform debris layers, we will further assume that the same compression formula holds in a differential sense such that $dL_m / dL_0 = (1/a)(dP/dL_0)^{-\gamma}$.

Fiber beds that are repeatedly cycled between high- and low-velocity flow experience successive compaction events whereby the preceding bed thickness is never fully recovered when the flow is reduced. This behavior is analogous to hysteresis phenomena and could be modeled as a damped oscillation if there were a pressing need to predict debris bed thickness for cycled flow conditions. However, to simplify the following data analysis, Eq. 14 will be applied only while pressure drop is increasing and the bed is under compression. When measurements indicate a decrease in pressure drop, bed thickness will not be allowed to increase. This means that compressive recovery is suppressed by assumption.

Total pressure reduction through a composite debris bed can be predicted by integrating Eq. 11 across the full bed thickness,

$$\Delta P = \frac{\rho^2 w_A^3}{\mu} \int_0^{\Delta L_m} \frac{b}{\varepsilon^3} Re^{m-1} dz. \tag{15}$$

When recast in the same terms as the compression correlation,

$$\left(\frac{\Delta P}{\Delta L_0}\right)^{-\gamma} = \left[\frac{\rho^2 w_A^3}{\mu \Delta L_0} \int_0^{\Delta L_m} \frac{b}{\varepsilon^3} Re^{m-1} dz\right]^{-\gamma} = a \frac{\Delta L_m}{\Delta L_0},$$

$$\vdots$$

$$\int_0^{\Delta L_m} \frac{b}{\varepsilon^3} Re^{m-1} dz = \frac{\mu \Delta L_0}{\rho^2 w_A^3}\left(a \frac{\Delta L_m}{\Delta L_0}\right)^{-\frac{1}{\gamma}}. \tag{16}$$

Equation 16 can only be true at the equilibrium bed thickness that will be established for a given debris arrangement having $\varepsilon(z)$ and $S_V(z)$, and distributed flow regime $Re(z)$. Equation 16 is also true regardless of the

pressure drop experienced. Iteration on composite bed thickness ΔL_m will yield the left-hand-side integral needed to evaluate final pressure drop using Eq. 15. Formulas given in the next section should be substituted during iteration to ensure that compression effects on porosity are fully coupled.

II. Composite Properties

Having established a complete parameterization of head loss in composite debris beds, including a description of compression in fiber dominated conditions, attention now turns to a discussion of material properties and the averaging formulas needed to describe the media. Section II.A discusses the surface-to-volume ratio S_V and its relationship to specific surface area, which can be measured independently. Values of S_V are provided for fiberglass. Section II.B discusses mixture porosity and its relationship to bed thickness. Limiting conditions are described and the generalized VISTA head-loss formula is expressed for any spatial arrangement of debris properties.

II.A. Surface-to-Volume Ratio

Debris beds commonly encountered on recirculation strainers for nuclear safety applications are always composed of a variety of constituents that are broadly classified into groups by shape (morphology) including: (1) particulates, (2) fibers, and (3) chips. Theoretical treatments of flow resistance (pressure drop) through debris beds include parameters that describe physical attributes of the debris using locally homogeneous parameters. The term locally homogeneous means that average properties preserve the characteristics of the bed over a spatial scale comparable to the random variation of the flow field – typically layers on the order of 5 to 10 diameters of the debris elements (50 to 100 μm). Local homogeneity does not preclude one-dimensional spatial variations through the bed. The common challenge for implementation of theoretical equations is to use knowledge about the quantity of debris, either mass or volume, and form descriptions of composite properties that are consistent with the theory.

The Ergun equation[5] and other derivations of flow in porous media based on microscopic phenomena are scaled to macroscopic flow conditions using a hydraulic radius defined in Eq. 4. Since the numerator $\varepsilon\forall$ is obviously the fraction of the total volume occupied by fluid, the complement $(1-\varepsilon)\forall$ must be the solid volume of debris. The ratio of debris surface area to debris solid volume, S_V $\left\{m^2/m^3\right\}$, is purely a parameter of convenience that is introduced to obtain wetted area in the denominator. It is important to understand that porosity ε and surface-to-volume ratio S_V are independent variables. This means that independently obtained values of each variable must be specified to fully describe flow conditions inside of a debris bed with fixed volume defined by ΔL_m. In essence, porosity describes the amount of empty space left in a bed and surface-to-volume ratio describes the area associated with solids that take up space. The relationship between surface area and volume is determined by the shape and size of the debris elements, which can be extremely complex.

The total solid volume of debris is easily computed if the material (microscopic) densities and masses are known for each constituent. Material density refers to the density of the most condensed physical elements of the debris material, which are much higher than the manufactured density of insulation composed of those materials. All insulation types contain a high fraction of void space to inhibit heat transfer. For example, the material density of the glass in fiberglass insulation is approximately 175 lbm/ft^3, but the manufactured density of the insulation is only 2.4 lbm/ft^3. Given the mass of constituents in the bed m_i and their respective material densities ρ_i^{mat}, the total solid debris volume is

$$V_{debris} = \sum \frac{m_i}{\rho_i^{mat}} = \sum \left(\frac{m}{\rho^{mat}} \right)_i . \tag{17}$$

The reciprocal of density $\upsilon = 1/\rho$ is a measurable debris property called specific volume $\left\{m^3/kg\right\}$ that leads directly to the formula for solid debris volume based on measured characteristics of individual constituents. A similar measurable property for debris surface area would lead directly to a formula for solid-debris surface area

$$A_{debris} = \sum m_i S_{Ai}, \tag{18}$$

where S_{Ai} is a legitimate specific surface area with units of $\left\{m^2/kg\right\}$. The solid area-to-volume ratio would then be

$$S_V = \frac{A_{debris}}{V_{debris}} = \frac{\sum m_i S_{Ai}}{\sum \left(m/\rho^{mat} \right)_i} . \tag{19}$$

Both the numerator and denominator of Eq. 19 can be expressed in terms of mass-weighted average properties without changing the composite value by dividing both numerator and denominator by the total mass $M_{debris} = \sum m_i$ to obtain

$$S_V = \frac{A_{debris}}{V_{debris}} = \frac{\sum m_i S_{Ai} / M_{debris}}{\sum \left(m/\rho^{mat} \right)_i / M_{debris}} = \frac{\sum w_i S_{Ai}}{\sum w_i \left(1/\rho^{mat} \right)_i} = \frac{\overline{S}_A}{\overline{\upsilon}},$$

where w_i are the mass fractions of each constituent in the bed, $\overline{S}_A$ is the mass-weighted-average specific surface area, and $\overline{\upsilon}$ is the mass-weighted-average specific volume. Mass-weighted composite properties are commonly used in all branches of science and engineering

as a matter of convenience because the mass of each constituent is so easily measured compared to any other physical property. The composite surface-to-volume ratio does not need to be factored or reduced any further than the expression $\overline{S}_A/\overline{\upsilon}$. The characteristic parameter S_V is simply the ratio of two summations over all debris in the bed for two different physical attributes.

Specific surface area S_A can be measured directly for various debris types and for composite mixtures using gas adsorption techniques attributed to Brunauer, Emmett, and Teller (BET). To determine the surface area, solid samples are pretreated by applying some combination of heat, vacuum, and/or flowing gas to remove adsorbed contaminants (typically water and carbon-dioxide) acquired from atmospheric exposure. The sample is then cooled under vacuum, usually to cryogenic temperature (77 K, -195 °C). An adsorptive (typically nitrogen or krypton) is then dosed to the solid in controlled increments. After each dose of adsorptive, the pressure is allowed to equilibrate and the quantity adsorbed is calculated. The quantity adsorbed at each pressure (and temperature) defines an adsorption isotherm, from which the quantity of gas required to form a monolayer over the external surface of the solid is determined. Theory predicts the area covered by each adsorbed gas molecule, so the total surface area can be calculated. Given the specific surface area, surface-to-volume ratio is then determined using best-available material densities and the formula $S_V = \rho^{mat} S_A$.

The extension of geometric surface-to-volume formulas to a composite mixture of debris elements with different shapes, but known individual masses and material densities, is straightforward

$$S_V = \frac{A_{solid}}{V_{solid}} = \frac{\sum S_{Vi}\left(m/\rho^{mat}\right)_i}{\sum\left(m/\rho^{mat}\right)_i} = \frac{\sum S_{Vi}\left(m/\rho^{mat}\right)_i}{V_{debris}} = \sum \nu_i S_{Vi},$$

where ν_i are the fractions of total solid volume contributed by each constituent. This formula demonstrates that when individual surface-to-volume ratios are known for each constituent debris element, the composite can be factored in the form of a linear volume-weighted average. If all specific volumes $\upsilon_i = 1/\rho_i$ are constant, the previous equation is equivalent to

$$S_V = \frac{A_{solid}}{V_{solid}} = \frac{\sum S_{Vi}\left(m/\rho^{mat}\right)_i}{\sum\left(m/\rho^{mat}\right)_i} = \frac{\upsilon}{\upsilon}\frac{\sum m_i S_{Vi}}{M_{debris}} = \sum w_i S_{Vi},$$

where the w_i are mass fractions for each constituent in the bed.

II.B. Mixture Porosity

Porous media composed of multiple constituents are typically treated as a homogeneous mixture with bulk averaged properties. Two of the most important properties are surface-to-volume ratio of the solid debris and porosity, or the amount of internal volume that permits fluid flow. Adding to the challenge is the fact that debris beds contain a variety of debris types, densities, shapes, sizes, and surface roughness factors, and the fact that fibrous debris beds compress under differential pressure. This section discusses the calculation of composite, or mixture, porosity.

The concept of composite porosity is easy to develop for a hypothetical example where there are only two debris types, like a single density of particulate and a single density of fiber. Debris of all types takes up space inside of a given volume of the porous bed, and the debris solid volume can be expressed in terms of both the "solidity", or solid fraction of the total volume, and the ratio of mass to material density:

$$\left(1-\varepsilon_m\right)\forall = \frac{m_f}{\rho_f^{mat}} + \frac{m_p}{\rho_p^{mat}} = \alpha_m \forall, \tag{20}$$

where ε_m is the porosity, α_m is the solidity, $\forall = A\Delta L_m$ is the total bed volume of cross sectional area A and thickness ΔL_m, and m_i and ρ_i^{mat} are the mass and material densities for particulate and fiber. Solving Eq. 20 for porosity gives

$$\begin{aligned}
\varepsilon_m &= 1 - \frac{1}{A\Delta L_m}\left(\frac{m_f}{\rho_f^{mat}} + \frac{m_p}{\rho_p^{mat}}\right), \\
\varepsilon_m &= 1 - \frac{1}{A\Delta L_m}\frac{m_f}{\rho_f^{mat}}\left(1 + \frac{m_p}{\rho_p^{mat}}\frac{\rho_f^{mat}}{m_f}\right), \\
\varepsilon_m &= 1 - \left(1 + \eta\frac{\rho_f^{mat}}{\rho_p^{mat}}\right)\frac{m_f}{\rho_f^{mat}}\frac{1}{A\Delta L_m},
\end{aligned} \tag{21}$$

where $\eta = m_p/m_f$ is the particle-to-fiber mass ratio.

The last two factors of Eq. 21 represent the ratio of fiber solid volume to total bed volume. If the fiber debris were considered as a debris bed by itself, it would have a characteristic solidity given by

$\left(1-\varepsilon_0\right)\forall_0 = \frac{m_f}{\rho_f^{mat}} = \left(1-\varepsilon_0\right)A\Delta L_0$. Here, the subscript $_0$ denotes a theoretical limit defined by the fiber-only bed response. Substituting this result in Eq. 21 gives

$$\varepsilon_m = 1 - \left(1 + \eta\frac{\rho_f^{mat}}{\rho_p^{mat}}\right)\left(1-\varepsilon_0\right)\frac{\Delta L_0}{\Delta L_m}. \tag{22}$$

This is the form of composite porosity given as Eq. (B-22) in Ref. 6. The theoretical (manufactured) porosity of fiberglass insulation is generally assumed to be $\varepsilon_0 = 1 - \rho_f^{mfc}/\rho_f^{mat} = 0.986$.

Equation 22 introduces two important concepts. First, the particle-to-fiber mass ratio η is easy to calculate from experimental data if filtration is complete and all of the material added to a test is resident in the debris bed. Second, the porosity is only well defined within a known

volume. Equation 22 is factored to express the finite volume as a comparison between a theoretical, fiber-only bed thickness ΔL_0 and the actual bed thickness ΔL_m, but regardless of the measure used, bed volume must be specified before porosity can be calculated.

The ratio of fiber density to particulate density requires additional thought for a composite bed of thickness ΔL_m that contains many types of particulates and fibers. An averaging process is required. Consider only the particulates that have a total mass of $M_p = \sum m_i$ and a total solid volume of $V_p = \sum \left(m / \rho^{mat} \right)_i$. One estimate of "average" material density is

$$\overline{\rho}_p^{mat} = \frac{M_p}{V_p} = \frac{\sum \left(m_p \right)_i}{\sum \left(m_p / \rho_p^{mat} \right)_i} \text{ and}$$

$$\overline{\rho}_f^{mat} = \frac{M_f}{V_f} = \frac{\sum \left(m_f \right)_i}{\sum \left(m_f / \rho_f^{mat} \right)_i}.$$

The ratio needed for Eq. 22 is then

$$\frac{\overline{\rho}_f^{mat}}{\overline{\rho}_p^{mat}} = \frac{\sum \left(m_f \right)_i}{\sum \left(m_f / \rho_f^{mat} \right)_i} \frac{\sum \left(m_p / \rho_p^{mat} \right)_i}{\sum \left(m_p \right)_i} = \frac{1}{\eta} \frac{\sum \left(m_p / \rho_p^{mat} \right)_i}{\sum \left(m_f / \rho_f^{mat} \right)_i},$$

which suggests that Eq. 22 can be written more concisely as

$$\varepsilon_m = 1 - \left(1 + \xi \right) \left(1 - \varepsilon_0 \right) \frac{\Delta L_0}{\Delta L_m}, \tag{23}$$

where ξ is the particle-to-fiber *volume* ratio

$$\xi = \frac{\sum \left(m_p / \rho_p^{mat} \right)_i}{\sum \left(m_f / \rho_f^{mat} \right)_i}. \tag{24}$$

It is often common to write porosity in terms of the complement solidity $\alpha = 1 - \varepsilon$ so that

$$\alpha_m = \left(1 + \xi \right) \alpha_0 \frac{\Delta L_0}{\Delta L_m}. \tag{25}$$

The final topic related to mixture porosity is bed compression, which clearly affects bed thickness through the last factor of Eq. 23 that in turn is defined by Eq. 16. In the limit of maximum compaction discussed in Section I.B, the bed will have a maximum packing density of about $c_{max} = 65$ lb$_m$/ft^3 (1041 kg/m^3). From Eq. 20, it is noted that the solidity can be expressed as the ratio of debris solid volume to total bed volume, so under maximum compaction

$$\alpha_{max} = \left(V_f + V_p \right) / V_{bed} = V_{debris} \frac{c_{max}}{M_{debris}} = \frac{c_{max}}{\overline{\rho}_{debris}^{mat}}, \tag{26}$$

where c_{max} is the maximum expected packing density (sometimes called the sludge limit) and $\overline{\rho}_{debris}^{mat}$ is the average material density of all debris elements. Given the maximum solidity, the minimum bed thickness can be obtained by solving Eq. 25 to obtain

$$\Delta L_{min} = \left(1 + \xi \right) \alpha_0 \frac{\Delta L_0}{\alpha_{max}}. \tag{27}$$

More problematic than the compression limit perhaps is the continuum of compression responses implied by Eq. 14. Equation 16 states the equilibrium condition that must exist between bed thickness and porosity given a parameterized correlation for fiber compression. The mixture porosity and complementary solidity from Eq. 23 and Eq. 25 are now substituted in Eq. (16) to obtain a statement of equilibrium that is explicit in ΔL_m and in the spatial arrangement of material properties;

$$\int_0^{\Delta L_m} \frac{b dz}{\left[1 - \alpha_0 \left(1 + \xi \right) \left(\Delta L_0 / \Delta L_m \right) \right]^3} \left[\frac{\rho w_A}{\mu S_V \alpha_0 \left(1 + \xi \right) \left(\Delta L_0 / \Delta L_m \right)} \right]^{m-1}$$

$$= \frac{\mu \Delta L_0}{\rho^2 w_A^3} \left(a \frac{\Delta L_m}{\Delta L_0} \right)^{-\frac{1}{\gamma}}. \tag{28}$$

Although the formula appears more complex, the essential nature of the iteration has not changed. Given spatial profiles of $S_V(z)$, $\xi(z)$, $b(z)$ and $m(z)$, iterate on ΔL_m until the equality is satisfied. This iteration is firmly bounded, so if no solutions are found within the range $\Delta L_{min} \le \Delta L_m \le \Delta L_0$, the limit having best agreement represents the desired equilibrium bed thickness.

III. Calibration to Head Loss Measurements

High-Temperature Vertical Loop (HTVL) data generally include several minutes of clean-strainer flow data that is collected prior to debris introduction. The strainer itself can be treated as a "porous" medium having a fixed porosity and a fixed surface-to-volume ratio. Fluid acceleration through the strainer plate persists as a background pressure loss in all debris data. Clean-strainer data can be used to correlate this loss and subtract it from total pressure drop data prior to correlation of the debris-bed behavior.

A series of tests was conducted for the South Texas Project (STP) Nuclear Operating Company[7] over a range of temperatures, flow velocity and bed characteristics. Derived drag coefficients for all flow conditions measured in all clean strainer conditions is shown in Fig. 2. The expected logarithmic behavior is clearly evident in the figure; however, variability in the ensemble of data leads to 20% variations between predictions and measured clean-strainer data for any single test. All clean strainer head losses fall in the range of 0.10 ft to 0.15 ft, depending on the dominant range of Reynolds number for

the test, so variation in this background is small compared to expected resistance induced by debris.

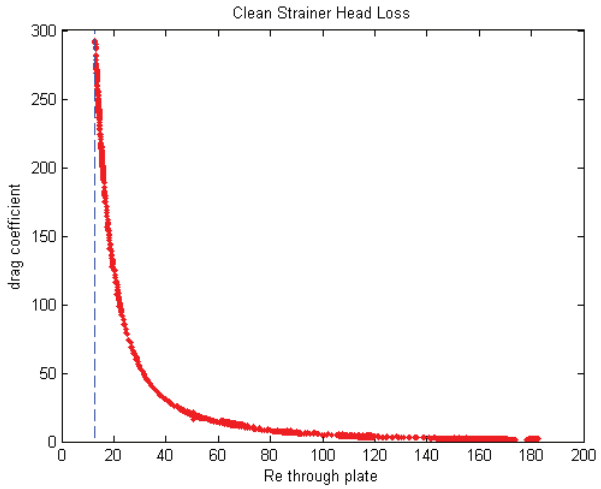

Fig. 2. Derived drag coefficient for all measured clean-strainer test data in perforated plate matching STP strainer construction.

Equation 16 provides a general formula for head-loss prediction that accommodates spatial variations in bed properties, but the model can be calibrated to data collected under homogeneous bed conditions where there is no severe influence from stratification and the bed properties are relatively well known. For uniform beds under uniform compression described by Eq. 15:

$$\frac{\Delta P}{\Delta L_0} = \frac{\rho^2 w_A^3}{\mu}\frac{b}{\varepsilon^3} Re^{m-1}\frac{\Delta L_m}{\Delta L_0}, \quad \vdots \quad \frac{\Delta P}{\Delta L_0} = \left[\frac{b}{a}\frac{\rho^2 w_A^3}{\mu\varepsilon^3}\left(\frac{\rho w_A}{\mu(1-\varepsilon)S_V}\right)^{m-1}\right]^{\frac{1}{1+\gamma}}. \tag{29}$$

Using HTVL test data for ΔP, Eq. (29) can be used to find least-squares, best-fit solutions for the unknown parameters b/a, $m-1$, and $1/(1+\gamma)$. Once these parameters are quantified over a range of Re, they can be applied in Eq. 16 to predict head-loss for any postulated debris configurations.

Nonlinear optimization techniques are required to simultaneously infer the compression parameters, so for this exercise, the standard recommend values $\tilde{a} = 1.3$ and $\gamma = 0.38$ are applied. It is further assumed that the fiber bed does not expand when the differential pressure decreases during the test. In other words, bed thickness is forced to be monotonically decreasing except when debris is being added.

STP Test 6 – Series 2, was chosen for initial calibration of the VISTA drag parameters because a very uniform debris bed was formed by adding 12 small batches of fiber and particles in constant proportion to borated-buffered aqueous solutions. Figure 3 illustrates the relatively complex temperature, velocity, and head-loss history experienced during the test. Figure 4 illustrates the viscosity and density traces that existed during the test. These properties were interpolated from NIST water tables using measured temperature. Although borated-buffered solution was used for all tests, test temperatures were also elevated above 50°C, indicating no need for any additional viscosity increase above pure water to account for background chemicals. Figure 5 illustrates the internal flow Reynolds number that changes as a function of flow conditions through the static bed. No information was available regarding the thickness of the debris bed, so standard parameters were assumed for the compression function with no additional constraints from observation. Figure 6 illustrates the bed thickness as a function of time that was found to be consistent with measured pressure drops that were selected to be monotonically increasing to emulate continuous compression with no relaxation.

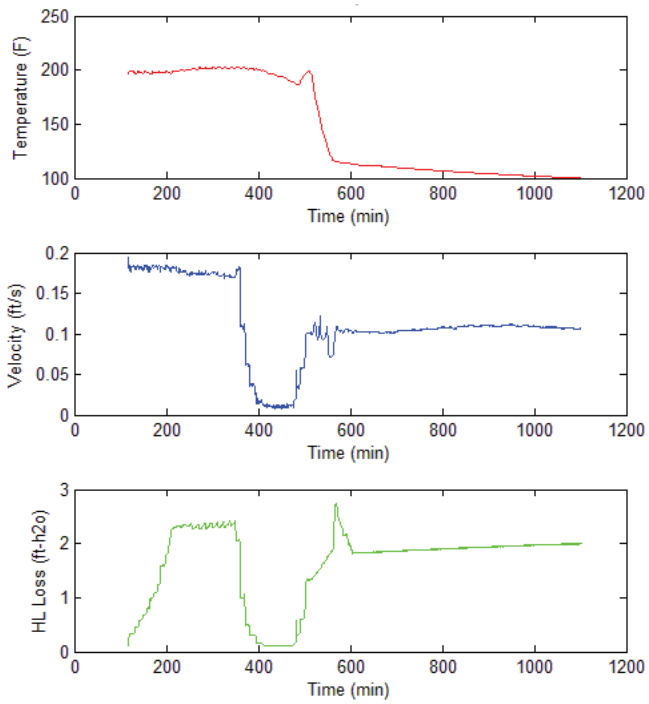

Fig. 3. Temperature, velocity and head-loss history experienced during test STP Test 6 - Series 2.

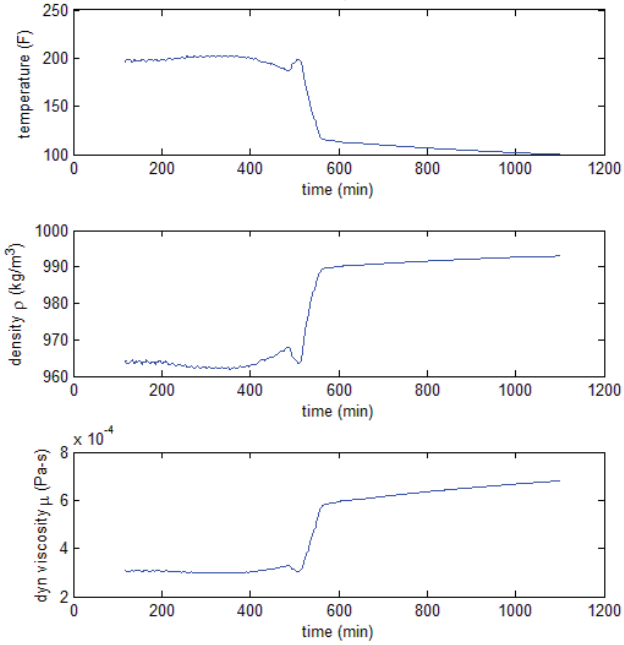

Fig. 4. Water properties existing during STP Test 6 – Series 2.

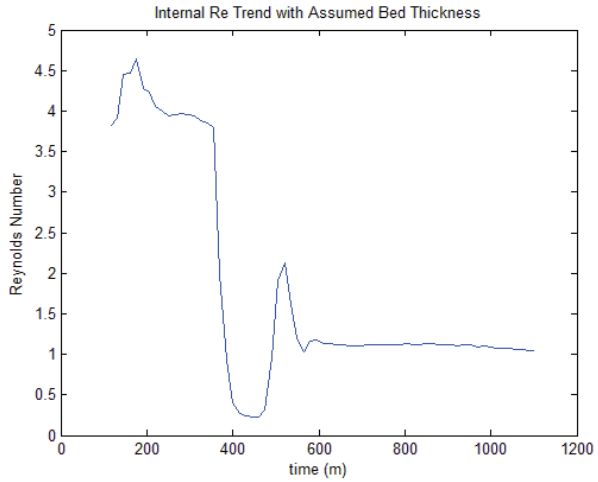

Fig. 5. Time-dependent internal flow Reynolds number during STP Test 6 – Series 2.

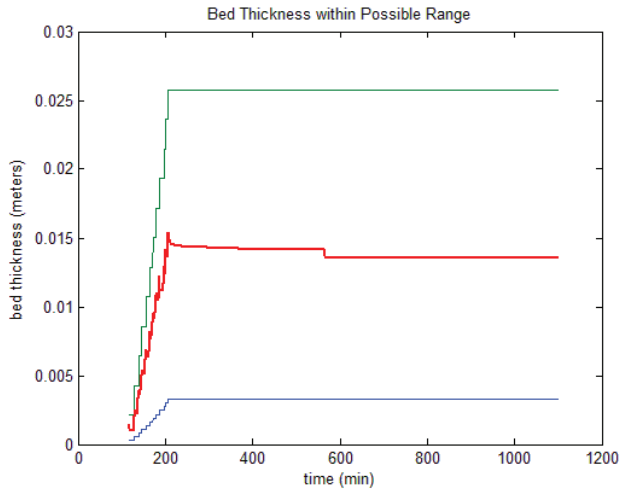

Fig. 6. Computed bed thickness (red) consistent with measured pressure between upper and lower theoretical limits.

Recall that the objective of the VISTA drag correlation is to collapse all factors of internal bed complexity onto the internal flow Reynolds number that is then used to index a low-order power law drag coefficient. A notional *a priori* trend for the drag law is shown in Fig. 1 with a region of expected interest where the drag function is essentially a straight line in log-log space. Figure 7 illustrates the remarkable agreement with expectation that is obtained by correlating data from the preceding plots for STP Test 6. Nearly linear (in log-log space) drag coefficients computed as $C_{drag}\left(Re\right) = bRe^{m}$ are obtained within a factor of 2 over exactly the Reynolds range expected. Best-fit coefficients from the calibration test are $b = 3.14$ and $m = -0.49$. Presumably, agreement would improve with use of a higher fidelity compression model and observational evidence to use as a constraint on maximum compression.

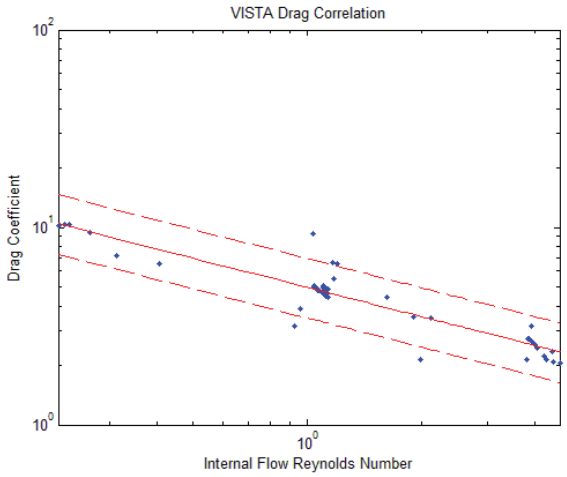

Fig. 7. VISTA drag correlation from single calibration test with uniform combination of fiber and acrylic paint particulate obtained using measured surface-to-volume ratios.

IV. Application to Composite Debris Beds

After all coefficients are determined for bed compression and for the VISTA drag correlation, spatial distributions must be assumed for debris properties within the bed so that predictive head-loss formulas can be evaluated to predict head-loss for a given fluid and flow regime. Head-loss prediction is complicated by the effect of iterative compression, which depends internally on the differential pressure. A two-step process requires that Eq. 16 be iterated to determine equilibrium bed thickness ΔL_m before Eq. (15) is integrated to obtain the desired prediction of ΔP . Bed thickness is determined by iterating the equilibrium formulas on the ratio $r_m = \Delta L_0 / \Delta L_m$ (see Ref. 1).

The largest single uncertainty in any head loss experiment is determining the bed thickness in tandem with corresponding pressure drop readings. Although bed composition can be determined to various degrees of accuracy, bed thickness, which controls porosity, is often unknown. Further complicating the determination of bed thickness is the high turbidity caused by suspended particulates introduced to the head-loss test.

Uniform bed properties were assumed to predict pressure drop for the calibration test using global VISTA parameters determined in the previous Section. Figure 8 compares the measured head loss to the head loss predicted using the two-step formulas given above for the calibration test. In this prediction, bed-thickness relaxation was not suppressed. Notice that after flow resumes at 500 min, the prediction underestimates the measurement because the standard compression formula has no awareness of prior compaction. During initial bed formation and pseudo steady-state flow (up to 400 min), the prediction shows good agreement with the measurement as illustrated in the Fig. 9 correlation plot. Dashed bands indicate factors of 1.5 above and below the diagonal line that represents perfect correlation.

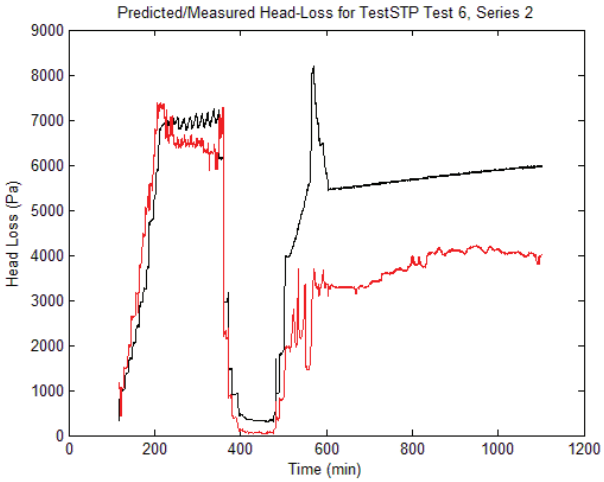

Fig. 8. Prediction of differential pressure history (red) compared to measurement.

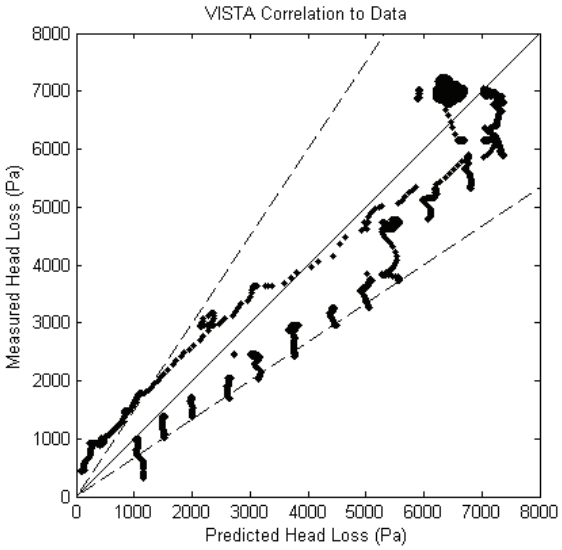

Fig. 9. Correlation of VISTA prediction to calibration data during initial bed formation and steady-flow operation.

Better agreement with the test history can be obtained by either imposing monotonic bed compression using the current model, adding hysteresis (damping term) to the current model, or reformulating compression based on a more complete theory of hydraulic drag. The important influence of compression and compaction is common to all head-loss formulas, but is outside the scope of the

current study. In a regulatory setting, for example, prediction of head loss on a sump strainer during a post-LOCA flow transient, it is common to adopt appropriately conservative parameterizations as long as they are benchmarked to relevant data and can be related to the range of variability induced by differences in bed formation and response to similar debris loads and flow conditions.

V. CONCLUSIONS

The Viscous Inertial Shear-Transition-Adaptive (VISTA) Porous Media Head-Loss Formulation shows promise for replacing traditional correlations that are cast as the sum of two concurrent physical processes that trade dominance over a wide range of flow conditions. When applied outside the range of calibration, the two-term formulas often behave like overfit polynomials yielding unpredictable results. The VISTA correlation supports a natural balance between viscous shear and inertial drag as supported by data in the range of interest while preserving theoretical limits identically. The VISTA model was developed specifically to treat performance of modern emergency core cooling system strainers that operate at low velocity and in a Reynolds flow regime that may span the viscous to inertial transition.

Other than preserving Reynolds scaling across the viscous to inertial transition, VISTA does not purport to explain the molecular kinetics that occur within the transition region. VISTA does, however, offer a more flexible algebraic combination of the two phenomena that may yield insights to deeper physical theories. For example, a fully calibrated VISTA parameterization sets an empirical constraint on the first derivative with respect to *Re* of any predictive model for drag within the transition region. Two-term approximations treat viscous and inertial forces as independent and additive with relative magnitude controlled by linear coefficients. VISTA uses Reynolds number to collapse the ratio of inertial force to viscous force into a fundamental scaling parameter that simplifies experimental testing and potentially reduces the number of free parameters.

Formulas presented here illustrate both the development of the basic head-loss gradient as well as application to beds comprising composite materials in any spatial arrangement. Although illustrated using a familiar fiber compression model, other treatments of compression and compaction may be more effective at describing bed compression and recovery. The example should serve as a guide for convenient implementation of any desired approximation.

More work remains to apply the formulation to high-quality head loss data containing well-controlled bed thickness to reduce uncertainties in bed porosity. In this respect, VISTA is similar to all correlations that depend on external macroscopic descriptions of internal bed characteristics. As with any model, proper calibration to measurements is required, but the effect of measurement uncertainty should be propagated to and reported with any required calibration constants. In this example, uncertainties on porosity imposed by assumed bed behavior dominate all direct measurement errors on temperature, differential pressure and flow rate, which are typically in the range of 1 to 3% for typical instrumentation.

The example analysis illustrates how VISTA can be calibrated for a single range of Reynolds number where the drag coefficient is essentially constant. The same process can easily be repeated over successive (and perhaps slightly overlapping) ranges of Reynolds number to fully characterize how the first derivative of the drag coefficient changes throughout the full viscous to inertial transition.

The goal of all physical models is to collapse apparent complexity onto a small number of scaling parameters that establish similitude across a spectrum of physical variations. In this application, VISTA uses Reynolds number to define commonality between interstitial flow regimes. Although Reynolds scaling is a familiar concept, more work is needed to establish the generality of a well-calibrated VISTA model and build confidence that identical interstitial Reynolds flow regimes can exist at different temperature, different velocity and different debris combinations.

ACKNOWLEDGMENTS

The authors are grateful to South Texas Nuclear Operating Company for financial support of this work and for the opportunity to develop explanatory models of complex phenomena.

REFERENCES

1. B. C. Letellier, M. E. Macali, and E. Kee, “Viscous Inertial Shear-Transition-Adaptive (VISTA) Porous Media Head-Loss Formulation for Assessment of the South Texas Project Licensing Amendment Request,” ALION-REP-STP-8998-11, Rev. 0, July (2014).
2. C. E. Lapple and C.B. Shepherd, *Calculation of Particle Trajectories*, Ind. Eng. Chem. 35(5), 605-617, May (1940).
3. W., Ingmanson, B. D. Andrews, and R. C. Johnson, Internal Pressure Distribution in Compressible Mats Under Fluid Stress, TAPI Journal 42(10), 840-849, (1959).
4. P. C., Carman (1997, reprint of original published in 1937, December, original published in May). Fluid Flow Through Granular Beds. Trans IChemE 75 (reprint of original Vol. 15), S32–S48 (reprint of original 1937 pages 150–166).

5. S. Ergun, Fluid Flow through Packed Columns, Chemical Engineering Progress, Vol. 48, No. 2, pp. 89-94, February (1952).
6. G. Zigler, J. Brideau, D. V. Rao, C. Shaffer, F. Souto, and W. Thomas, Parametric Study of the Potential for BWR ECCS Strainer Blockage Due to LOCA Generated Debris, NUREG/CR-6224, prepared for the U. S. Nuclear Regulatory Commission by Science and Engineering Associates, Inc., Albuquerque, NM, October (1995).
7. ALION-REP-STP-8511-02, South Texas Vertical Loop Head Loss Testing Report. Revision 1 January (2013).